Molecular and Cellular Neuroscience 83 (2017) 13–26

Contents lists available at ScienceDirect

Molecular and Cellular Neuroscience

journal homepage: www.elsevier.com/locate/ymcne

Cutaneous inflammation regulates THIK1 expression in small C-like nociceptor dorsal root ganglion neurons

William Haskins [a,1], Sergio Benitez [b], Juan M. Mercado [b], Cristian G. Acosta [b,*]

[a] School of Physiology, Pharmacology and Neuroscience, Faculty of Biomedical Sciences, University of Bristol, BS8 1TD, UK
[b] Instituto de Histologia y Embriologia de Mendoza (IHEM), Facultad de Medicina, Universidad Nacional de Cuyo, 5500 Mendoza, Argentina

ARTICLE INFO

Article history:
Received 3 February 2017
Revised 29 June 2017
Accepted 30 June 2017
Available online 1 July 2017

Keywords:
THIK1
K2P
Dorsal root ganglia
Sensory neurons
Pain
Cutaneous inflammation

ABSTRACT

Tandem pore-domain Halothane Inhibited K^+ channel (THIK1) is a two-pore-domain potassium channel (K2P) present in dorsal root ganglia (DRG). We previously demonstrated that THIK1 mRNA levels in the DRG dropped ipsilaterally 1 day after CFA-induced cutaneous inflammation (CFA1). In this study we aimed to identify the currently unknown DRG subpopulations expressing THIK1, and to investigate the relationship between the channel and both inflammatory and spontaneous pain in normal rats. Using a combination of immunohistochemistry, western blotting and behavioural tests, we found that all small neurons and large groups of medium and large DRG neurons express THIK1. Myelinated and unmyelinated fibers, nerve endings in the skin and lamina I and II of the spinal cord also express the channel. THIK1 staining co-localizes with IB4-binding and trkA suggesting that the channel is expressed by nociceptors. At CFA1, both cytoplasmic and edge (membrane-associated) THIK1 staining were significantly reduced only in small neurons ipsilaterally compared to normal. At 4 days after inflammation (CFA4), edge THIK1 staining levels in small neurons decreased bilaterally compared to normal. Medium and large size DRG neurons showed no change in THIK1 expression either at CFA1 or CFA4. Ipsilateral (but not contralateral) mean %intensities of THIK1 in small neurons at CFA1 correlated strongly negatively with spontaneous foot lifting (SFL) duration (a marker of spontaneous pain). Thus, nociceptors express THIK1 that can be regulated by cutaneous inflammation. Finally, *in vivo* siRNA knockdown of THIK1 resulted in longer SFL duration than siRNA scramble-treated rats. Taken together our evidence suggests a potential involvement for THIK1 in pain processing following inflammation.

1. Introduction

Pathological and acute pain of peripheral origin can arise from partial nerve injury, tissue damage and/or inflammation. Changes in the electrophysiological properties of primary afferent neurons of the dorsal root ganglia (DRG) are essential for the initiation and maintenance of this pain. For example, alteration of soma membrane potential (Em) in A- and C-fiber nociceptors can be seen *in vivo* (Djouhri et al., 2012). The causes of these changes are only partly understood. In models of inflammatory and pathological pain the reported changes involve increased spontaneous firing (SF) rate, spontaneous foot lifting (SFL) and/or lowered nociceptive sensory and electrical thresholds in intact fibers (Djouhri et al., 2006; Wu et al., 2001; Wu et al., 2002).

Given their contribution to setting up Em, K^+ channels have recently been recognized as potential new targets for the treatment of refractory and pathological pain (Ocana et al., 2004; Tsantoulas, 2015; Tsantoulas and McMahon, 2014; Wood, 2007). Leak K^+ channels of the 2-pore domain family (K2Ps) are key contributors to resting Em and thus regulate cell excitability making them of particular relevance for the control of pain (Busserolles et al., 2016; Du et al., 2014; Mathie and Veale, 2015). In fact, DRG neurons express several K2P channels that are involved in neuroprotection, nociception and mechanotransduction. For example, TRESK knockout and axotomy both enhance DRG neuron excitability (Tulleuda et al., 2011), and a dominant negative TRESK mutation is implicated in familial migraine (Lafreniere et al., 2010). Further, we recently demonstrated that TREK2 expressed selectively in IB4-binding nociceptors limits spontaneous pain (Acosta et al., 2014). TREK2 is also involved in the response to non-aversive warm and moderate cool temperatures (Pereira et al., 2014).

THIK1 (Tandem pore-domain Halothane Inhibited K^+ channel) is amongst the least studied K2P channels. THIK1 is encoded by the KCNK13 gene and was first described in conjunction with its closely

Abbreviations: DRG, (dorsal root ganglion); THIK, (Tandem pore domain Halothane Inhibited K^+ channel); K2P, (2-pore domain K^+ channels); CFA, (Complete Freund's Adjuvant); trkA, (TRK1-transforming tyrosine kinase protein); NGF, (nerve growth factor); TREK2, (TWIK-related K^+ channel 2); TASK, (TWIK-related acid-sensitive K^+ channel).

* Corresponding author.
E-mail address: cacosta@fcm.uncu.edu.ar (C.G. Acosta).
[1] Present address: Department of Clinical Neuroscience, School of Medicine, Southampton University, SO17 1BJ, UK.

http://dx.doi.org/10.1016/j.mcn.2017.06.010
1044-7431/

related partner, THIK2. When expressed in mammalian cell lines, THIK1 produced a large sustained K^+ current, was activated by high levels of arachidonic acid and inhibited by halothane (Rajan et al., 2001). THIK1 is expressed by a variety of tissues including arterial endothelium (Bryan et al., 2006), kidney (Theilig et al., 2008) and in neurons of the retrotrapezoid nucleus (Lazarenko et al., 2010) and the trigeminal ganglia (Kang et al., 2014). In the latter, THIK1 contributes to the background K^+ conductance, showing a small unitary conductance (~5 pS), and is inhibited ~80% by cold (10 °C) (Kang et al., 2014). In our previous study, we demonstrated that THIK1 mRNA levels in the DRG were lower 1 day after Complete Freund's adjuvant (CFA) induced cutaneous inflammation (CFA1) when compared to normal (untreated) rats and levels were higher at CFA4 compared to CFA1 (Marsh et al., 2012). Although on the surface these findings suggest an involvement of THIK1 in inflammation, several key questions remain unanswered regarding its possible role in pain processing. These include: what subpopulations of DRGs normally express THIK1, does expression change after CFA-induced cutaneous inflammation, and does a relationship exist between THIK1 and inflammation-induced spontaneous pain behavior.

Accordingly, we used a combination of immunohistochemistry, western blotting and behavioral tests to examine the expression pattern of THIK1 in adult normal DRGs classed by size and the overlap with phenotypic markers (NF200, IB4 and trkA). We then examined whether expression of this channel changes 1 and 4 days after cutaneous inflammation induced by CFA and whether such changes are related to spontaneous pain behavior.

2. Materials and methods

2.1. Animals

All Methods complied with both Home Office (United Kingdom) Guidelines and all animals were cared for in accordance with the Guiding Principles in The Care and Use of Animals of the US National Institute of Health. All procedures were approved by the Institutional Animal Care and Use Committee of the School of Medical Sciences, Universidad Nacional de Cuyo (Protocol approval N° 31/2014). A total of 40 young female Wistar rats (140–160 g) were used throughout. Animals were culled at the end of experiments with an overdose of anesthetic (80 mg/kg ketamine plus 10 mg/kg xylazine).

2.2. Primary antibodies

2.2.1. THIK1 antibody characterization

Anti-THIK1 antibody (RRID: AB_10612227) was an affinity-purified rabbit polyclonal from Santa Cruz Biotechnology (Z-21, sc-134,086). Western blots of IMR-32 whole cell lysate suggest this antibody is selective for THIK1 (Santa Cruz website).

Additionally we examined its selectivity for THIK1 *versus* the closely related THIK2 and another K2P channel, TASK2. All aforementioned K2P channels were heterologously expressed in HeLa cells (Fig. 1a). Three separate cultures of HeLa cells were grown in DMEM containing 10% FBS until they reached 60–80% confluence. Next they were co-transfected with rat cDNAs encoding for the different K2P channels and GFP using Attractene (Qiagen) following the manufacturer's instructions. These cells were chosen because their native expression of most K2P channels is either undetectable or very low. THIK1, THIK2 and TASK2 were sub-cloned in pCMV-SPORT. All plasmids were sequenced to confirm the correct reading frame. Co-transfection with pAc-GFPN1 (Clontech) was used because it allowed us to detect which HeLa cells were more likely to have been transfected.

Three days after transfection, the HeLa cell cultures expressing the different K2P channels were washed with PBS, fixed with 4% paraformaldehyde plus 4.2% sucrose (in PB, pH 7.2) for 20 min at 4 °C, rinsed with PBS and then immediately processed for THIK1 immunocytochemistry as described below. This antibody proved selective for THIK1 *versus* the other transfected K2Ps. We performed a Western Blot analysis of HeLa transfected cells alongside a variety of other tissues (Fig. 1b–c).

Finally, we undertook further antibody characterization using selective knockdown of THIK1 expression with siRNA in adult DRG cultures. DRGs from all rostrocaudal levels were dissected out (Acosta et al., 2012; Acosta et al., 2014). Briefly, they were enzymatically digested at 37 °C in 0.25% trypsin with 0.625% collagenase in PBS, mechanically dissociated, plated onto round coverslips (Bellco, Germany) coated with 10 ng/mm^2 poly-D-Lysine and kept in DMEM supplemented with N2 medium at 37 °C in a 5% CO_2 incubator until used. Neuron density at plating was ~1×10^5 neurons/ml.

Dissociation and the culture process are equivalent to a form of acute axotomy, leading to deprivation of normally available target-derived, and nerve-derived, trophic factors. Trophic factor supplements are therefore required to maintain a relatively normal phenotype *in vitro*. Thus, cultures were supplemented with mouse NGF7S (10 ng/ml) and rat recombinant GDNF (20 ng/ml) (Preprotech, UK). Both were dissolved in 0.1% BSA and were added daily with fresh N2 medium.

siRNA Silencer Select was obtained from Ambion (Life Technologies Ltd., UK). 6 h after plating, DRG neurons were transfected with 5 nM scrambled (scr) siRNA conjugated to 5′-carboxylfluorescein (FAM), or with10nM siRNA directed against rat THIK1 (KCNK13, locus ID 64120, *sense* 5′-CUCCCAUCUUGUAACUAAAtt-3′; antisense 5′-UUUAGUUACAAGAUGGGAGct-3′) plus 5 nM scr-FAM (to allow identification of likely transfected cells). Transfection was performed with Gene Silencer siRNA transfection reagent (Genlantis, San Diego, CA) following the manufacturer's protocol. We have used this transfection system before and it works well in cultured DRG neurons (Wu et al., 2006; Acosta et al., 2014). Subsequent daily medium changes included 10 nM naked THIK1 siRNA.

Fluorescence microscopy at 2 days *in vitro* showed which neurons were transfected with the non-targeting FAM-labeled scr siRNA (Fig. 1e), indicating that these neurons were probably also successfully transfected with THIK1 siRNA.

2.2.2. Other antibodies and IB4 staining

For double labelling studies, we used staining with Isolectin B4 (IB4), which labels small, C-nociceptor neurons in the DRG (Fang et al., 2006). We also used the following phenotypic markers: RT97 (RRID:AB_528399, DSHB, Iowa University, deposited by JN Wood) a mouse monoclonal antibody against a highly phosphorylated form of the 200 kDa neurofilament (NF200) subunit, that selectively labels DRG neuron somata with myelinated A-fibers (Lawson et al., 1984; Lawson et al., 1993). A goat affinity purified anti-trkA from R&D Systems (RRID:AB_2154974) that has been fully characterized (Acosta et al., 2014; Usoskin et al., 2015) and a guinea pig affinity purified anti-Substance P from Neuromics (GP14110, RRID: AB_2315368) that has been extensively used in the literature. For specific staining of nerve terminals, a mouse anti-β tubulin III antibody was used (clone SDL.3D10, Cat# ab11314 RRID:AB_297918).

2.3. Western blot

Total protein was extracted from either 72 h transected-HeLa cells, whole cerebellum, kidney, heart, liver, spinal cord and L4/L5 DRGs or skin (from the *in vivo* siRNA experiments, see Section 2.8) using Laemmli buffer supplemented with Halt protease and phosphatase inhibitor cocktail (Thermo Scientific). Samples of ~20 μg of total protein were run in 8–10% PAGE gels and transferred to a PVDF membrane before blotting. Membranes were probed with 1:500 rabbit anti-THIK1 antibody and then with 1:1000 mouse anti-α-tubulin (clone DM1A, eBioscience) as a loading control. Membranes were developed using ECL-plus and captured with Image Quant LAS-4000 (GE Healthcare).

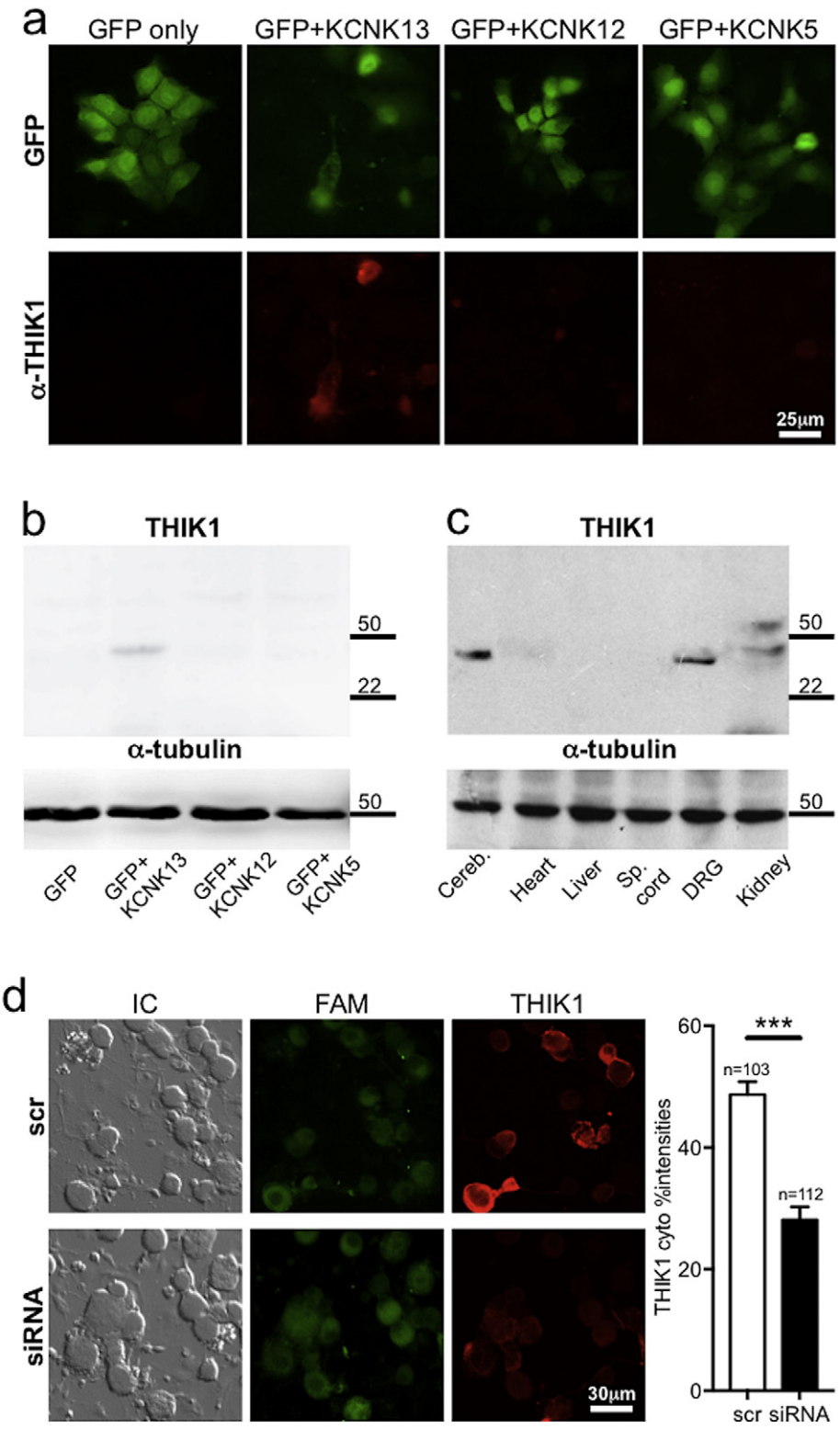

Fig. 1. THIK1 antibody characterization (**a**) Top panels show GFP fluorescence in HeLa cells transfected with plasmids for GFP alone and 3 rat K2P channels indicated by their genes: THIK1 (*KCNK13*), THIK2 (*KCNK12*) and TASK2 (*KCNK5*) (all subcloned in pCMV-SPORT vector). Lower panels: same fields show no immunostaining for THIK1 in HeLa cells transfected with GFP alone, increased substantially following transfection with THIK1 cDNA and remained very low or undetectable after transfection with the non-THIK1 K2P channels tested. This antibody therefore selectively recognizes THIK1 and not the other K2P channel tested, including THIK2, structurally the closest related to THIK1. (**b**) Western blot analysis of HeLa cells transfected as described in (a) shows a single band only when the cells were transfected with the plasmid encoding the cDNA for *KCNK13*. (**c**) Representative Western blot showing the expression of THIK1 protein from whole cerebellum (lane 1), heart (lane 2), liver (lane 3), spinal cord (lane 4), DRG (lane 5) and kidney (lane 6). Approximately 20 μg of protein were run in each lane of SDS-PAGE gels mouse α-tubulin was used as loading control. The WB shows that the anti-rabbit polyclonal antibody used detects a single band of approximately 46 kDa. Molecular weight ladder is included to the right of the blot. (**d**) In adult DRG neurons cultured with NGF plus GDNF for 2 days, THIK1 siRNA reduced THIK1 staining (bottom), compared with scr (top). Photomicrographs (×20 objective). For quantification of these 2-day cultures, only transfected neurons were measured (those with >20% FAM cytoplasmic staining). THIK1 cytoplasmic staining intensity was highly significantly decreased (Mann-Whitney test, $p < 0.001$) with THIK1 siRNA compared with scr treatment. These studies show selectivity of the THIK1 antibody in DRG neurons.

2.4. Induction of cutaneous inflammation

Cutaneous inflammation in one hind limb was induced under anesthesia (25 mg/kg ketamine plus 5 mg/kg xylazine i.p.), by intradermal injection of 100 μl Complete Freund's Adjuvant (CFA) (Sigma) into the mid-plantar surface of the left hindpaw as previously described (Acosta et al., 2014; Acosta et al., 2012). DRG tissue was removed from one group of four rats after 24 h (CFA1) and from a further four rats 4 days after CFA injection (CFA4). Four normal (untreated) rats were used as absolute control. Intradermal CFA injection is a well-characterized method of generating inflammatory pain-related behavior associated with increased activity in nociceptors (Djouhri et al., 2006; Millan, 1999). Comparisons of the effects of CFA-induced inflammation are made with both, the contralateral side of the CFA-injected rats and normal (untreated) rats throughout. Note that contralateral DRGs may be affected due to the known global (*i.e.* systemic) effects of locally induced inflammation (Jancalek et al., 2011; Koltzenburg, 1999).

The choice of times (1 and 4 days) after CFA injection is based on studies in rat that showed both spontaneous firing (SF) in nociceptors and spontaneous foot lifting (SFL) were greater at 1 day, and lower at 4 days (Djouhri et al., 2006).

2.5. Immunocytochemistry

2.5.1. Immunofluorescence on cultured DRG neurons and HeLa cells

After fixation with 4% paraformaldehyde and 4.2% sucrose cells were permeabilized for 4 min with 0.2% v/v Triton X-100 in PBS, blocked for 2–3 h at room temperature with 1% bovine serum albumin plus 5% foetal calf serum and then incubated overnight at 4 °C with anti-THIK1 (1:400) diluted in the blocking solution. On the next day, coverslips were washed with PBS and incubated for 1 h at room temperature with 1:800 donkey anti-rabbit Alexa 594 (Molecular Probes), washed again and mounted with FluorSave (Calbiochem).

For each transfection condition, images of 6 fields were captured at 40× (HeLa) or 20× (DRG cultures) magnification under fluorescence illumination.

2.6. Immunohistochemistry

2.6.1. Tissue preparation

Four untreated, four CFA1 and four CFA4 rats were used for the quantification study. For the *in vivo* siRNA experiment, twenty additional rats were used (four as controls and sixteen treated, see Section 2.8). Rats deeply anesthetized with 50 mg/kg ketamine plus 10 mg/kg xylazine i.p. and transcardially perfused with 0.9% NaCl followed by Zamboni's fixative (Stefanini et al., 1967). Skin, sciatic nerve and spinal cord and L5 DRGs were then dissected and post-fixed for 20 min in Zamboni's at RT and then kept in 30% sucrose overnight at 4 °C. The following day serial 7 μm cryostat DRG (transverse) sections were cut. This tissue was kept at −20 °C until used for immunoassay.

2.6.2. ABC immunostaining

Mid-sections of L5 DRGs were processed for staining against THIK1 (antibody used at 1:400) using the avidin-biotin complex (Elite ABC kit, Vector labs) immunocytochemistry method following previously published protocols (Acosta et al., 2014; Fang et al., 2006). 3,3′-diaminobenzidine (DAB) was used to generate a coloured reaction product. No staining resulted in the absence of the primary antibody. All sections were developed simultaneously and for the same length of time to enable comparisons of relative staining intensity.

2.6.3. Immunofluorescence

For double or triple immunofluorescence staining of L5 DRG sections from 4 normal (untreated) rats, skin, sciatic nerve or spinal cord, mid-cryosections of 5–7 μm were rehydrated with PBS for 10 min and then permeabilized 5 min with 0.2% v/v triton-×100 and blocked for 1 h at RT with 5% BSA. Anti-THIK1 (1:400) staining was performed overnight at 4 °C followed by rinsing with PBS and incubation 1 h at room temperature with a donkey anti-rabbit Alexa 488 (1:800). After rinsing of the secondary antibody with PBS, sections were incubated overnight at 4 °C with either mouse anti-NF200 (RT97, 1:4000), goat anti-trkA (1:2000), goat anti-SP (1:1000), mouse anti-β-tubulin III (1:2000) or IB4-conjugated to Alexa-594 (1:500). On the next day, sections incubated with RT97 or anti-trkA were incubated for 1 h at room temperature with a goat anti-mouse 594 antibody (1:800) and in the case of triple immunofluorescence, also with DAPI (1:1000), then washed and mounted with FluorSave. Images were captured with a Nikon 80i microscope and stored for offline analysis.

2.6.4. Image analysis

In vivo, we measured both the relative intensities of cytoplasmic and edge immunostaining for THIK1. *In vitro* we only examined whole cytoplasmic staining to assess the specificity of THIK1 antibody using siRNA-induced knockdown of THIK1. Cytoplasmic levels are indicative of the overall available protein including newly synthesized channels. It is also the way most studies reported ion channel expression in the DRG, and thus, our measurements allow for direct comparison with previously published studies. We also measured THIK1 mean pixel densities at the edge of the cytoplasm up to the membrane (referred to hereafter as edge) as this likely reflects the levels of the channel close to or in the plasma membrane, where it is presumably active. We have used a similar approach to measure membrane-associated (edge) staining for TREK2 (Acosta et al., 2014), alpha3-Na^+/K^+-ATPase (Parekh et al., 2010) and HCN1/HCN2 (Acosta et al., 2012) in DRG sections. All measurements were made using HCImage software. We measured the same number of mid-sections of the L5 DRG in each rat and condition. Only neurons with a clearly visible nucleus were measured. Our sampling method assured that the number of small, medium and large neurons we measured faithfully represent the proportions of such neurons in the adult rat DRG. The average cytoplasmic pixel density (designated ***c***) over the whole cytoplasm excluding the nucleus was measured. Then within the same section, the minimum neuronal cytoplasmic staining (***a***, 0%) was determined as the average cytoplasmic pixel density of the three least stained neurons, and the maximum cytoplasmic staining was the average pixel density of the three neurons with densest cytoplasm (***b***, 100%). Percentage relative intensity of cytoplasmic staining was obtained as follows: Relative intensity $= 100 \times ((\boldsymbol{c} - \boldsymbol{a}) / (\boldsymbol{b} - \boldsymbol{a})$. The same procedure was repeated to determine trkA and IB4 cytoplasmic relative intensities. Based on our previously published data using immunostaining in *in vivo* dye-injected neurons, we considered any staining %intensity equal to or larger than 20% above background as positive (Acosta et al., 2014; Acosta et al., 2012; Fang et al., 2005; Fang et al., 2006). In the same images, we measured edge relative pixel density within a carefully drawn line (examples of cytoplasmic and edge measurements are shown as masks in Supplementary Fig. 1S). These are also presented as percentages relative to the above minimum (background) and maximum total mean cytoplasmic values (**a** and **b**).

2.7. Spontaneous foot lifting (SFL)

SFL was observed at CFA1 and CFA4. Observations were completed within ~1 h prior to DRG harvest. SFL was measured after exploratory, grooming behavior and locomotion had ceased and the rat was stationary on all four paws (for details see (Djouhri et al., 2006; Yoon et al., 1996)). SFL was the cumulative duration of time (in seconds) for which the rat elevated the ipsilateral hindpaw, measured over two 5 min intervals. In the case of siRNA knockdown experiments (see Section 2.8) we also report the number of events of SFL during the 10 min period. Due to ongoing inflammation, this SFL was often accompanied by foot shaking/licking or other aversive behavior. The contralateral (untreated) hindpaw showed no SFL. Normal (untreated) rats do

not show SFL. The duration of SFL has been shown to positively correlate with rate of C-fiber firing, rather than being secondary to allodynia (Djouhri et al., 2006).

2.8. In vivo siRNA knockdown of THIK1

THIK1 was knocked down *in vivo* following our previously successful protocol for TREK2 (Acosta et al., 2014). At day 0, a single 2 μg dose of rat THIK1-specific siRNA (see Section 2.2) or scr siRNA, with the cationic polymer transfection reagent *in vivo*-jetPEI™ (Polyplus-transfection SA, Illkirch, France), was injected intradermally into the left hindpaw of 20 female Wistar rats. Neither these injections nor this transfection reagent caused any detectable inflammatory response in our experiments. Three days later, rats were injected at random with either saline (4 rats) or CFA (16 rats); SFL duration and SFL number of events were examined 24 h later. Although local biosynthesis in afferent A and C-fibers/terminals occurs for some molecules *e.g.* (Asante et al., 2009) it is not known whether THIK1 synthesis occurs only in neuron somata or also in their fibers. The timing we used (4 days after siRNA/scr injection) allowed transport time for any knockdown in the soma to influence fiber THIK1 levels and this timing would thus also probably allow knockdown of any THIK1 expression that may occur within the fiber. As it was the case for TREK2 in our previous study using this approach, we predicted that down-regulation of THIK1 after THIK1 siRNA in fibers innervating the injected region would occur by 4 days after siRNA injection *i.e.* 1 day after the CFA injection.

The efficacy of the *in vivo* THIK1 knockdown by siRNA was evaluated by Western blot and immunocytochemistry (representative examples of these are shown in Fig. 8) after SFL measurement, *i.e.* 4 days after siRNA/scr and 1 day after CFA. For the evaluation, rats were deeply terminally anesthetized (80 mg/kg Ketamine plus 10 mg/kg xylazine). Skin tissue was harvested for protein extraction and Western Blotting within 2 h of completing the behavioral tests. These rats were then immediately perfused with fixative, for removal of tissues (additional skin and proximal nerves innervating the skin). Immunocytochemistry was then performed on frozen sections of skin and sciatic nerve (see Section 2.6).

2.9. Statistical tests

All statistical comparisons of subgroups of neurons were non-parametric due to small numbers in groups, or groups failing the D'Agostino-Pearson normality test. Results are shown as means ± SEM and comparison of means were with Kruskal-Wallis for three groups (solid lines indicate groups tested), with Dunn's *post hoc* tests between all combinations of groups. Correlations were with the non-parametric Spearman correlations (Spearman's correlation coefficient, r_s, given where significant). All tests were performed with Prism 7 (GraphPad software). Tests were 2-tailed and a level of $p < 0.05$ was considered statistically significant. Significance is indicated on all graphs by $^{*}p < 0.05$, $^{**}p \le 0.01$, $^{***}p \le 0.001$, $^{****}p \le 0.0001$.

3. Results

3.1. THIK1 antibody characterization

The polyclonal THIK1 antibody that we used throughout was Z-21 (RRID: AB_10612227, Santa Cruz Biotechnology). Fig. 1a shows that this antibody recognizes heterologously expressed THIK1 (KCNK13) but not the structurally, closely related THIK2 (KCNK12) nor the other K2P channel tested (TASK2, KCNK5), indicating high selectivity for THIK1. Fig. 1b shows that this antibody also recognizes a band of the expected molecular weight (~46 kDa) in whole protein extracts from HeLa cells transfected with KCNK13 cDNA but not in those transfected with the closely structurally related KCNK12 (THIK2) or KCNK5 (TASK2). The antibody also recognizes a single band in protein extracts from cerebellum (lane 1), heart (weak, lane 2), DRG (lane 5) and kidney (lane 6) but not from liver or spinal cord (lanes 3 and 4 respectively) (Fig. 1c). This pattern of expression coincides with reports in the literature (Enyedi and Czirjak, 2010; Ishii et al., 2010; Theilig et al., 2008). Finally, we show that the anti-THIK1 antibody detected a significant reduction in the expression of THIK1 in 2 days *in vitro* cultured adult DRG neurons treated with a selective THIK1 siRNA compared to scr (as a negative control) (Fig. 1d).

3.2. THIK1 is expressed differentially by neurons according to size

Supplementary Fig. 1 shows a representative image of THIK1 ABC immunostaining in normal L5 DRG and two masks illustrating examples of the regions of interests (ROI) drawn in HCImage to allow quantification of cytoplasmic and edge immunointensities. Note that a mask is created for cytoplasmic measurements and then, on the same cells, a new mask is created to measure the edge pixel densities. Small neurons (≤400 μm^2, black arrowheads) are strongly stained for THIK1 unlike large neurons (≥800 μm^2, black arrows) that show little or no staining. There is also some visible peripheral (not cytoplasmic) staining in glial cells.

DRG neurons with cytoplasmic and edge %intensities (*i.e.* relative percentages of maximum) of THIK1 ≥ 20% were classed as THIK1 +, and those with <20% as THIK1- (see Section 2.6.4). Edge levels are assumed to reflect membrane associated staining and therefore expression of active channels. Cytoplasmic levels are also used as they better reflect total synthesis of the channel but additionally permit comparison with other studies on the expression of channels *in vivo*, such as Nav1.8, HCN1 and 2, TREK2 etc. published by our own group. Image analysis of 206 neurons from L5 midsections obtained from 4 normal rats showed that both THIK1 cytoplasmic and edge %intensities were significantly and negatively correlated with cell area (Spearman's correlations were $r_s = -0.46$ and -0.39, $p < 0.0001$, for cytoplasmic and edge respectively, Fig. 2a–c). Mean ± SEM percentages of cytoplasmic *vs.* edge THIK1 for small, medium and large DRG neurons were 60.3 ± 1.9% *vs.* 58.7 ± 2.1% (n = 121), 42.7 ± 3.3% *vs.* 42.5 ± 3.2% (n = 51) and 27.0 ± 3.6% *vs.* 33.1 ± 3.4% (n = 34) respectively (Fig. 2d–e). Mean cytoplasmic and edge %intensities were not significantly different within each neuronal size group (Fig. 2f). Thus, DRG neurons of all sizes express THIK1 but most small neurons were THIK1 + and displayed the greatest THIK1 staining, followed by medium size neurons. With ~50% positively stained for THIK1, large neurons demonstrated the least staining.

3.3. IB4-binding (IB4 +) and trkA + DRG neurons express THIK1

To establish what subpopulation of DRG neurons expressed THIK1 we carried out double immunofluorescence staining of the channel and known phenotypic markers. First we examined whether neurons rich in neurofilament of 200 kDa (NF200) expressed THIK1. These neurons have been shown to have myelinated A-fibers (Lawson et al., 1984). Fig. 3a shows that in most large neurofilament-rich neurons there is no visible THIK1 cytoplasmic staining above background level. A few large NF200 + neurons exhibited weak cytoplasmic THIK1 staining (asterisk in Fig. 3a) which was also visible in myelinated fibers (Figs. 3f and S2b). Further, some THIK1 edge staining was observed in most neurofilament-rich neurons likely reflecting a degree of functional channel expression. Thus, at least some A-fiber neurons expressed THIK1 albeit at levels lower than those seen in unmyelinated, putative C-fiber DRG neurons (see Figs. 2d–e).

Almost all small neurons were positively stained for THIK1. Accordingly we next examined whether its expression was restricted to the IB4-binding (IB4 +) subpopulation. We found that cytoplasmic %intensities of THIK1 and IB4 were weakly positively correlated (Spearman's correlation $r_s = +0.24$, $p < 0.01$, Fig. 3b). The co-localization between THIK1 + and IB4 + (≥20% maximum IB4 staining, see Methods) staining was relatively poor: 48.5% of 103 THIK1 + neurons were IB4 +. On

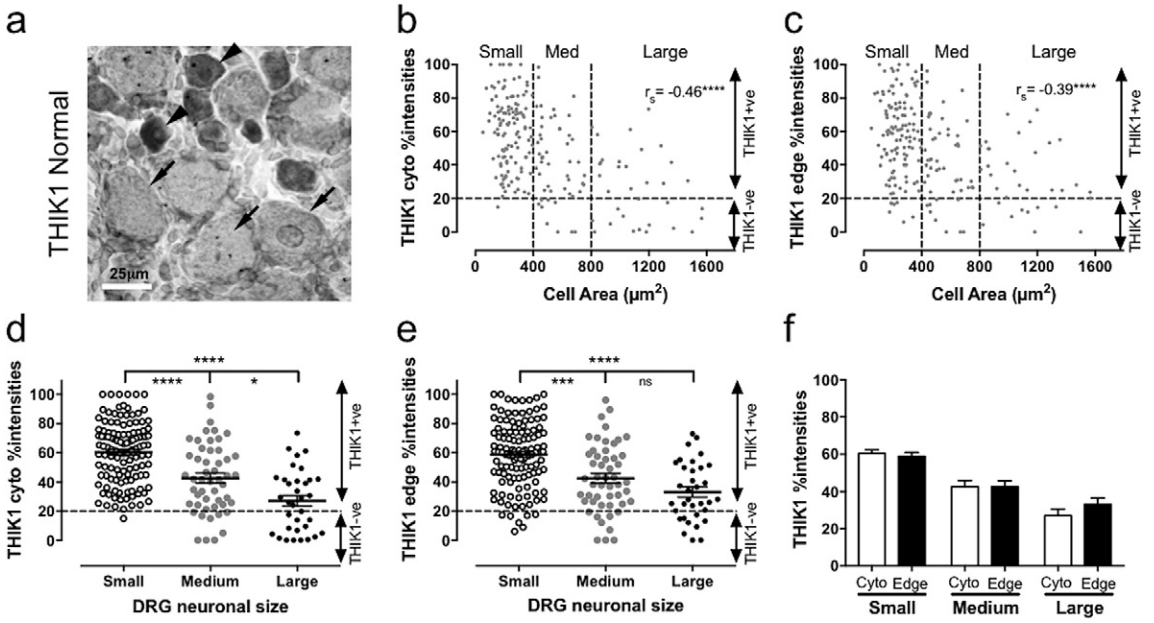

Fig. 2. THIK1 immunostaining in normal DRG (**a**) THIK1 typical ABC immunostaining with ×40 objective. Black arrowheads indicate examples of small DRG neurons with strong THIK1 staining. The arrows point to negatively stained medium and large size neurons. Plots show a significant negative Spearman's correlation between cross-sectional area and THIK1 cytoplasmic %intensities (**b**) and edge %intensities (**c**) of L5 DRG neurons (n = 4 rats). Neurons are classed as small (≤400 μm^2), medium (400–800 μm^2) and large (≥800 μm^2). Cells with cytoplasmic intensities below 20% were considered negatively stained for THIK1. Plots show THIK1 cytoplasmic %intensities (**d**) and edge %intensities (**e**) for small, medium and large DRG neurons in the L5 DRG of adult female Wistar rats. (**f**) Mean cytoplasmic and edge %intensities were not significantly different within each neuronal size group. Means ± SEM are shown for each neuronal subpopulation classed by size. Significance is indicated in all plots by $^*p \le 0.05$, $^{**}p \le 0.01$, $^{***}p \le 0.001$ and $^{****}p \le 0.0001$.

the other hand, the proportion of IB4+ and IB4- neurons that were THIK1+ were 77.4 and 84.4%, respectively. This indicates that THIK1 is expressed in similar proportions in both subgroups. It was previously shown that IB4+ DRG small neurons are C-fiber nociceptors in rat while a few weakly IB4+ medium sized (>400 μm^2) neurons were D hair units (Fang et al., 2006). Thus, about half of the THIK1+ DRG neurons in rat, being small and IB4+, are probably non-peptidergic C-fiber nociceptors.

THIK1 showed significant co-expression with trkA, the high affinity NGF receptor: 72.1% of 61 THIK1+ neurons were trkA+. Most neurons were stained for THIK1 (green) and trkA (red) (Fig. 3c). There was a significant and positive correlation between them (Spearman's correlation $r_s = +0.73$, $p < 0.001$, Fig. 3c). We only observed a very few large THIK1+/trkA+ neurons, which suggest that these were Aβ-nociceptors. We next examined whether THIK1+ neurons also co-localized with substance P, a known marker of peptidergic nociceptors that is also expressed by ~78% of trkA+ neurons (Kashiba et al., 1996). We observed that most THIK1+ small neurons indeed expressed SP (indicated by arrows in Fig. 3d) but, we found no SP+ large neurons, which is not surprising given that only 10% of A-fiber neurons express SP normally and none of those are Aα/β (McCarthy and Lawson, 1989). We also examined whether THIK1 was expressed in the periphery and centrally. We found THIK1 expression in the sciatic nerve, which co-localized partly with IB4 (Fig. 3e) and with RT97, a marker of myelinated fibers (Fig. 3f). This pattern was also recognizable by the presence of the typically large, elongated nuclei of Schwann cells (Radtke et al., 2005) (Figs. S2b and 8c). Nerve terminals in the skin were also stained positively for THIK1 (Fig. S2a). Therefore, THIK1 is expressed in both, IB4+ and trkA+/SP+ neuronal subpopulations and their fibers. Accordingly, we observed profuse THIK1 expression in the lamina I and II of the spinal cord, where the channel co-localized with both SP and IB4 (Fig. S2c,d). These observations suggest the possibility that THIK1 may be regulated by inflammation; a condition that involves pain responses mediated by IB4-binding and trkA+ neurons. Thus, we next examined whether THIK1 expression was regulated by cutaneous CFA-induced inflammation.

3.4. CFA-induced cutaneous inflammation alters THIK1 expression in DRG neurons

Due to our previous report of changes in THIK1 mRNA levels after cutaneous inflammation (see Introduction), we next examined a) whether THIK1 expression was altered in L4/L5 DRG neurons in a pain model and b) whether its expression was associated with spontaneous foot lifting (SFL), a measure of spontaneous pain. We choose the Complete Freund's Adjuvant (CFA) model for various reasons. First, it is simpler to study immunohistochemically than the 7-days spinal nerve axotomy (SNA) or the modified SNA (mSNA) models. In all these models intact DRG neurons are "inflamed" *i.e.* subject to inflammatory influences (Acosta et al., 2014; Djouhri et al., 2001; Djouhri et al., 2012; Watkins and Maier, 2002). However, in the SNA and mSNA models of nerve injury ~20–40% of ipsilateral L4 DRG neurons have axotomised/damaged fibers (Djouhri et al., 2006). This means that the L4 DRG contains a mixture of inflamed and axotomised neurons. Because phenotypic changes in inflamed and axotomised neurons often go in opposite directions (Djouhri et al., 2001), histological studies of their ipsilateral L4 DRG neurons are hard to interpret. Second, spontaneous firing in C-nociceptors increased by day 1 but recovered by day 4 after CFA-induced cutaneous inflammation (Acosta et al., 2014; Djouhri et al., 2001).

Thus, in this study we examined how THIK1 expression changed in small, medium and large neurons from L4/L5 DRG from 4 adult rats after 1 or 4 days subcutaneous injection of CFA (refer to as CFA1 and CFA4) compared with untreated rats (normal). THIK1 expression at the contralateral side of the same CFA-treated rats was also examined. There were differences in the appearance of ipsilateral and contralateral THIK1 immunostaining at CFA1 (Fig. 4a) and for ipsilateral at CFA4 (Fig. 5a) compared with untreated rats (normal).

At CFA1 the changes included significantly lowered cytoplasmic staining ipsilaterally in small neurons compared with both normal (untreated) and contralateral, with little or no change in medium and large neurons (Fig. 4b). THIK1 levels at the edge were significantly lowered both contra and ipsilaterally compared to normal, again with no

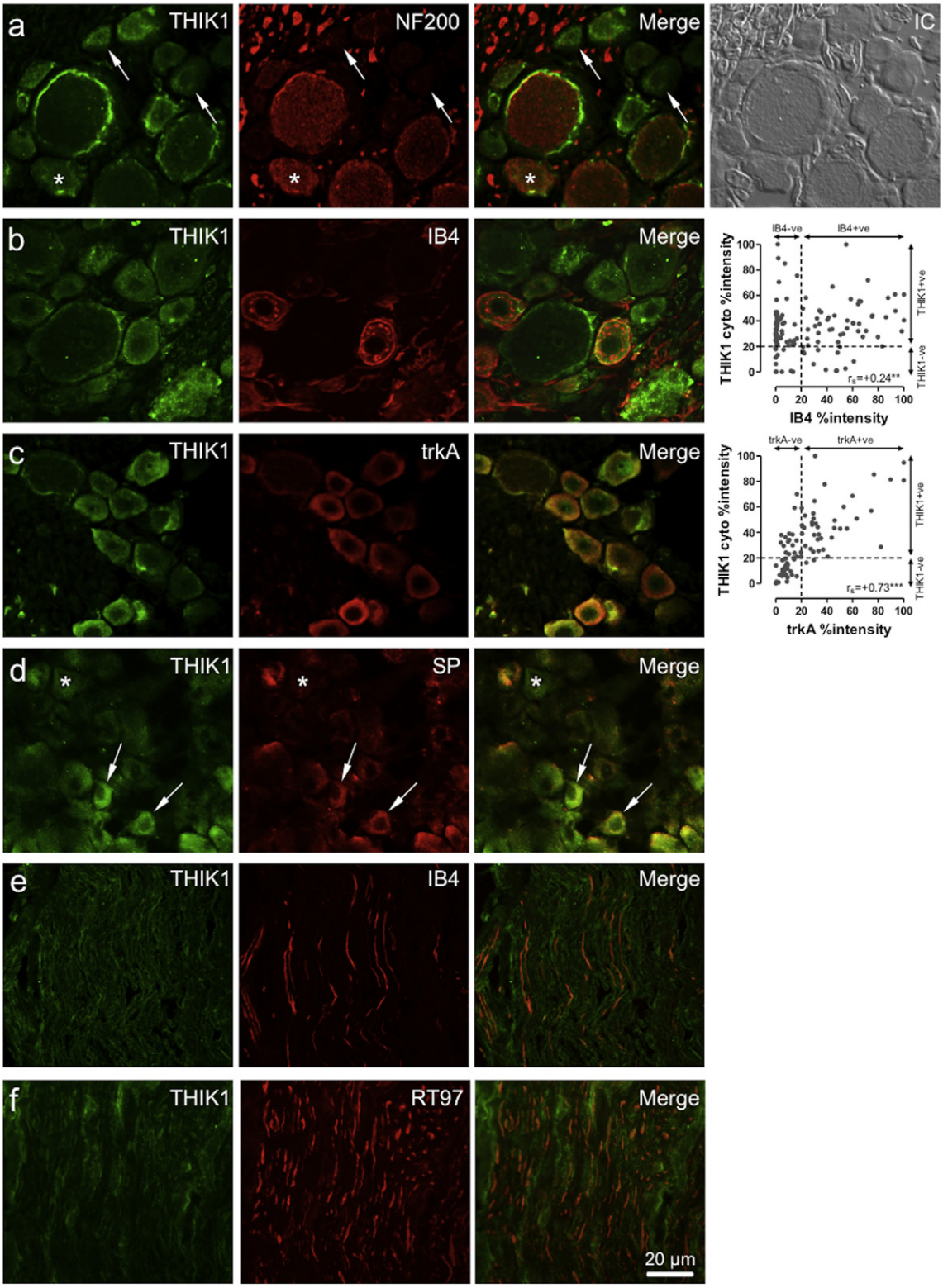

Fig. 3. THIK1 co-localization with DRG phenotypic markers (**a**) Cystoplasmic THIK1 staining (green) is present only in a few in large, myelinated, neurofilament-rich (RT97+, red) neurons (asterisk) but most RT97+ display some edge THIK1 staining. There is cytoplasmic THIK1 staining in RT97-, unmyelinated, small neurons (fine white arrows). (**b**) THIK1 staining (green) with IB4 conjugated to Alexa 594 (red) show that THIK1 cytoplasmic staining is evident in small neurons with strong IB4 staining. Spearman's correlation analysis (far right plot) shows that THIK1 cytoplasmic %intensities are positively but weakly correlated with IB4 cytoplasmic %intensities. (**c**) Representative photomicrographs of THIK1 immunostaining (green) and trkA (red). Most THIK1+ neurons are also trkA+. Spearman's correlation shows that cytoplasmic immunostaining for THIK1 is strongly and positively correlated with that of trkA. For statistical significance, see Methods. (**d**) Photomicrographs shows that THIK1+ small neurons (green) co-localize with SP+ neurons (red) in the L5 DRG (examples are indicated by arrows), suggesting that some THIK1+ neurons are peptidergic C-nociceptors. There were also a few small THIK1+/SP- neurons (indicated by an asterisk). (**e**) Longitudinal sections of sciatic nerve show abundant THIK1 staining that partly overlaps with IB4 binding. (**f**) THIK1 (green) is also present in myelinated fibers (stained with RT97, red). (**a**–**c**): All images captured at 40× magnification, (**d**) at 20× and (**e**,**f**) at 60× magnification. Yellow is indicative of overlapping expression. (For interpretation of the references to colour in this figure legend, the reader is referred to the web version of this article.)

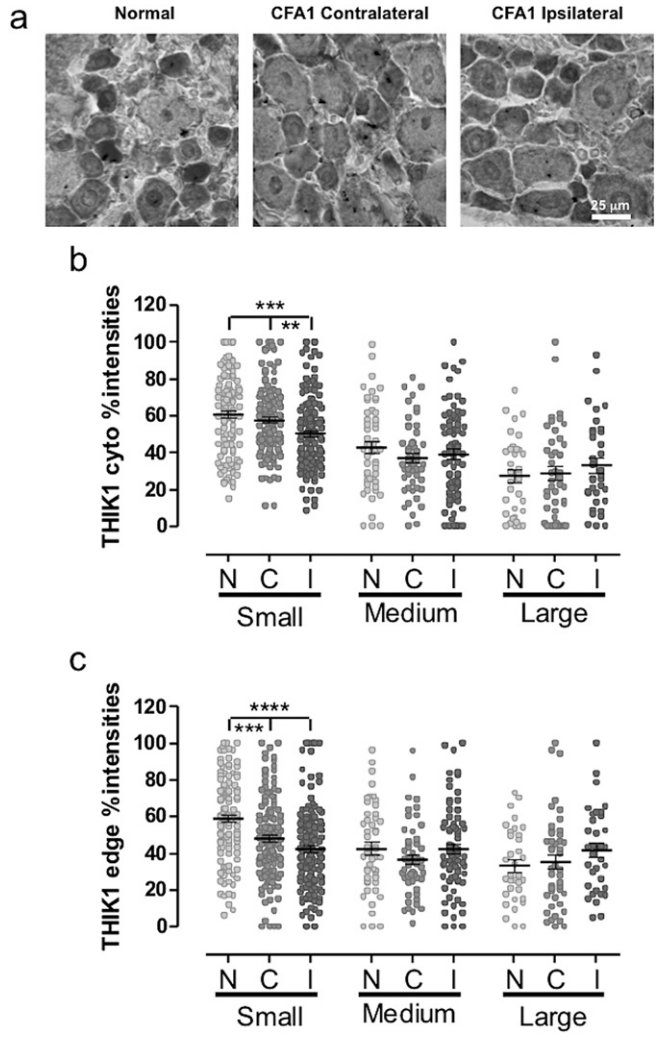

Fig. 4. THIK1 immunointensities 1 day after inflammation (**a**) Representative images of ABC/DAB THIK1 staining in normal (untreated), contra- and ipsilateral L5 DRG 1 day after CFA-induced cutaneous inflammation (CFA1). Note the reduction in the overall bilateral staining of small neurons with no change in medium and large neurons at this time. (**b**) Neurons subdivided into small, medium and large (cross sectional areas with nuclear profiles of ≤400μm^2, 400–800 μm^2, ≥800 μm^2 respectively). The scatter plot shows a comparison of cytoplasmic staining in sections of normal (N) L5 DRGs *versus* contralateral (C) and ipsilateral (I) L5 DRGs at CFA1. (**c**) A scatter plot showing a comparison of cell edge staining in the same neurons as described in (b). For each group, mean ± SEM are shown. Multiple comparisons done with ANOVA of N, I and C groups within each size range with Tukey's *post-hoc* test between each possible pair. For significances see Fig. 1 legend.

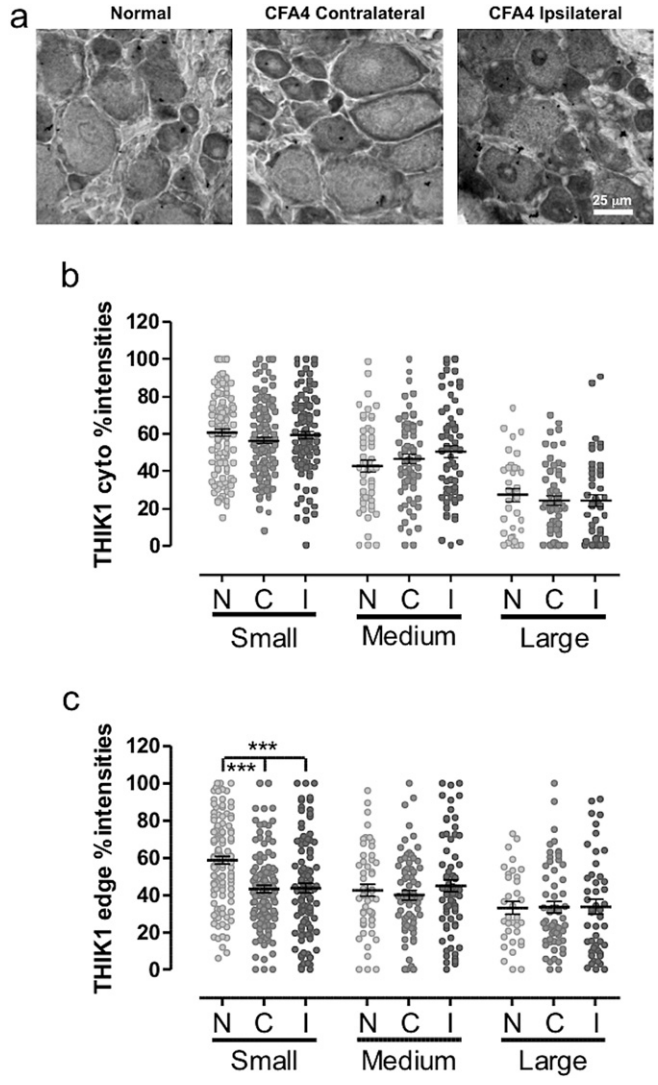

Fig. 5. THIK1 immunointensities 4 days after inflammation (**a**) Representative images of ABC/DAB THIK1 staining in normal, contra- and ipsilateral L5 DRG 4 days after CFA-induced cutaneous inflammation (CFA4). Note that overall, neurons of all sizes show ipsilaterally increased THIK1 staining intensity compared to normal (untreated) rats. (**b**) Neurons subdivided into small, medium and large (cross sectional areas with nuclear profiles of ≤400μm^2, 400–800 μm^2, ≥800 μm^2 respectively). The scatter plot shows cytoplasmic staining in sections of normal (N) L5 DRGs, contralateral (C) and ipsilateral (I) L5 DRGs at CFA4. (**c**) A scatter plot showing a comparison of cell edge staining in the same neurons as described in (b). For each group, mean ± SEM are shown. Multiple comparisons ran with ANOVA of N, I and C groups within each size range with Tukey's *post-hoc* test between each possible pair. Significance is indicated by $^*p \le 0.05$, $^{**}p \le 0.01$ and $^{***}p \le 0.001$.

significant changes either in medium or large neurons (Fig. 4c). This pattern is similar to the one we described for changes in THIK1 mRNA levels at CFA1, where the effects were also bilateral (Marsh et al., 2012). Notice that the drop ipsilaterally in THIK1 levels was more pronounced at the edge (17.7%) than in the whole cytoplasm (10.2%) compared to normal rats.

In contrast, at CFA4 we observed no significant changes in the cytoplasmic THIK1 immunostaining for any neuronal size. In fact, ipsilateral THIK1 was not significantly different from normal for small neurons. We observed a slightly (not significant) increased THIK1 cytoplasmic %intensities ipsilaterally in medium neurons compared to normal, while in large neurons both contra and ipsilateral levels were similar to normal (Fig. 5b). Interestingly, and similarly to what happened at CFA1, THIK1 edge %intensities were significantly and bilaterally lowered compared to normal rats. The drops were similar for contralateral (15.6%) and ipsilateral (15%). There were no significant differences in the THIK1 edge levels for either medium or large neurons (Fig. 5c).

Fig. 6 summarises our findings. The changes we observed ipsilaterally were significant or highly significant (Kruskal-Wallis, Dunn's *post-hoc* test, $p < 0.05$) compared with untreated (normal) rats. In small neurons, the mean % (±SEM) cytoplasmic staining in untreated (N), CFA1 (1) and CFA4 (4) were 60.3 ± 1.9 (n = 121), 50.1 ± 1.7 (n = 145) and 59.2 ± 2.1 (n = 102) respectively. For medium neurons the corresponding values for N, 1 and 4 were 42.7 ± 3.3 (n = 51), 39.1 ± 2.7 (n = 81) and 50.3 ± 3.2 (n = 68). Finally, for large neurons the mean % (±SEM) for N, 1 and 4 were 27.0 ± 3.6 (n = 34), 32.8 ± 4.1 (n = 35) and 24.1 ± 3.3 (n = 47) respectively. These data show that THIK1 cytoplasmic levels dropped significantly ipsilaterally in small neurons at CFA1 recovering by CFA4. There is also a modest increment in medium size neurons ipsilaterally at CFA4 compared to CFA1 but not different from the levels seen in untreated rats (Fig. 6a).

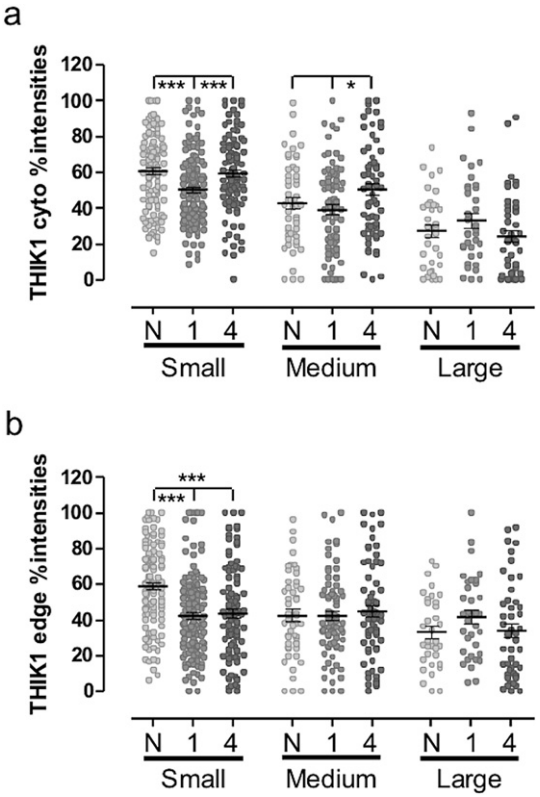

Fig. 6. Summary of the inflammation-induced changes in THIK1 immunostaining (**a**) Comparison of THIK1 cytoplasmic %intensities (staining) in sections of normal (N) L5 DRGs with ipsilateral L5 DRGs at CFA1 (1) and CFA4 (4) (**b**) Comparison of edge THIK1 %intensities in sections of normal (N) L5 DRGS with ipsilateral L5 DRGs at CFA1 (1) and CFA4 (4). Neurons subdivided into small, medium and large as in previous plots. Mean ± SEM are shown. Comparisons were made using ANOVA of N, 1 and 4 groups within each size range with Tukey's *post-hoc* test between each possible pair. Significance is indicated by $^{*}p \le 0.05$, $^{**}p \le 0.01$ and $^{***}p \le 0.001$.

THIK1 mean edge %intensities (±SEM) values for N, 1 and 4 in small neurons were 58.7 ± 2.1 (n = 121), 42.4 ± 1.9 (n = 145) and 43.7 ± 2.6 (n = 102) respectively. For medium neurons the corresponding values for N, 1 and 4 were 42.5 ± 3.2 (n = 51), 42.1 ± 2.5 (n = 81) and 45.0 ± 3.2 (n = 68). For large neurons the percentages for N, 1 and 4 were 33.1 ± 3.4 (n = 34), 41.5 ± 3.9 (n = 35) and 33.7 ± 3.9 (n = 47) respectively. Thus, THIK1 edge levels dropped significantly ipsilaterally compared to normal in small neurons only, an effect that was maintained from CFA1 through CFA4. There were no significant differences for medium and large neurons (Fig. 6b).

3.5. THIK1 expression and spontaneous pain at CFA1 & CFA4

The final question we addressed was whether the extent of spontaneous pain behavior (measured as SFL duration) was related to either ipsilateral or contralateral DRG neuron THIK1 cytoplasmic and edge levels (*i.e.* immunoreactivity) in the CFA pain model. We found that ipsilateral but not contralateral mean THIK1 cytoplasmic and edge %intensities in small neurons significantly and negatively correlated with SFL duration at CFA1 (Fig. 7a). This means that lower average levels of THIK1 expression in small DRG neurons occurred in rats that showed longer SFL durations, thus suggesting a possible involvement of this channel in spontaneous pain. This correlation was absent in medium and large DRG neurons ipsilaterally and in all neuronal sizes contralaterally (Supplementary Fig. S3). Note that THIK1 expression levels vary amongst animals (as we also observed for TREK2) suggesting that the extent of spontaneous pain would also be variable.

At CFA4 we found strong positive and significant correlations with SFL duration for a) mean cytoplasmic %intensities ipsilaterally in small neurons; b) ipsilaterally for both, mean cytoplasmic and edge %intensities in medium neurons and c) ipsilaterally for mean cytoplasmic %intensities in large neurons (Fig. 7b and Supplementary Fig. S4). So, at this time point greater THIK1%intensities correlates with more pain, not less as one might expect. However it must be noted, the duration of SFL at CFA4 is largely reduced in comparison to those recorded at CFA1, suggesting that spontaneous pain is far less intense at this later time (Djouhri et al., 2006). Nonetheless, correlation analysis suggested the distinct possibility that THIK1 is in some part involved in spontaneous pain. We next tested this hypothesis further, by examining the effect of decreasing THIK1 expression *in vivo* on this inflammation-induced SFL.

3.6. Selective THIK1 knockdown in vivo increases spontaneous pain behavior

Plantar intradermal THIK1 siRNA was injected *in vivo* 3 days prior to intradermal CFA or saline injection in the same region; SFL duration and number of events was measured at CFA1, *i.e.* 4 days after the siRNA (or scr-vehicle) injection (see Section 2.8). Rats received either CFA or saline at random. Fig. 8a shows that the siRNA treatment knocked down THIK1 effectively (2 rats shown here), while scr had no effect compared to either saline or CFA1 alone. The average drop in THIK1 expression with siRNA compared to saline was ~50% ($p < 0.01$) (Fig. 8b). In the proximal section of the nerve innervating ipsilateral plantar skin, IB4 + (red) and IB4- fibers clearly express THIK1 (green) after scr treatment; in contrast after 3 days with THIK1 siRNA these fibers had very low THIK1 after CFA treatment (Fig. 8c). Thus THIK1 siRNA treatment resulted in clearly decreased THIK1 expression.

CFA injection caused increased SFL duration and number of events whether preceded by scrambled siRNA or THIK1 siRNA ($p < 0.001$). However, the latter showed a moderately higher level of SFL than the former ($p < 0.05$) (Fig. 8d). This increase in SFL duration and number of events in rats with THIK1 knockdown, although mild, is consistent with THIK1 contributing to spontaneous pain.

4. Discussion

This is the first demonstration that THIK1 is widely expressed amongst DRG neurons. Almost all small neurons and a substantial subpopulation of medium and large neurons express the channel. THIK1 co-localizes with IB4 + and trkA + neurons *in vivo* suggesting this channel is largely expressed by nociceptors, although NF200 staining suggests possible low-level THIK1 expression in low threshold mechanoreceptors (LTMs) also. Accordingly, THIK1 expression is present in both, myelinated and unmyelinated fibers in the sciatic nerve and also in the nerve terminals innervating the skin. Further, we show that CFA-induced cutaneous inflammation downregulates THIK1 expression in small neurons selectively at different times. We also report that at CFA1 mean ipsilateral THIK1 cytoplasmic and edge %intensities in small DRG neurons correlated significantly and negatively with SFL duration (a measure of spontaneous pain). At CFA4 we found comparatively reduced SFL durations that correlated positively with THIK1%intensities. Finally, selective *in vivo* knockdown of THIK1 slightly (but significantly) increased SFL at CFA1. Overall, our evidence suggests that THIK1 may be involved in pain processing during inflammation.

4.1. Identity of THIK1-expressing neurons

When investigating THIK1 cytoplasmic immunoreactivity we found staining is particularly intense in DRG neurons classed as small according to their cross-sectional area at the nuclear level (≤400 μm^2). These small DRG neurons are unmyelinated, slowly conducting and are thought to be mostly C-fiber nociceptors (Lawson, 2002; Lawson et al., 1993; Lawson and Waddell, 1991). A comparatively smaller, but still substantial proportion of medium and large neurons are also positively

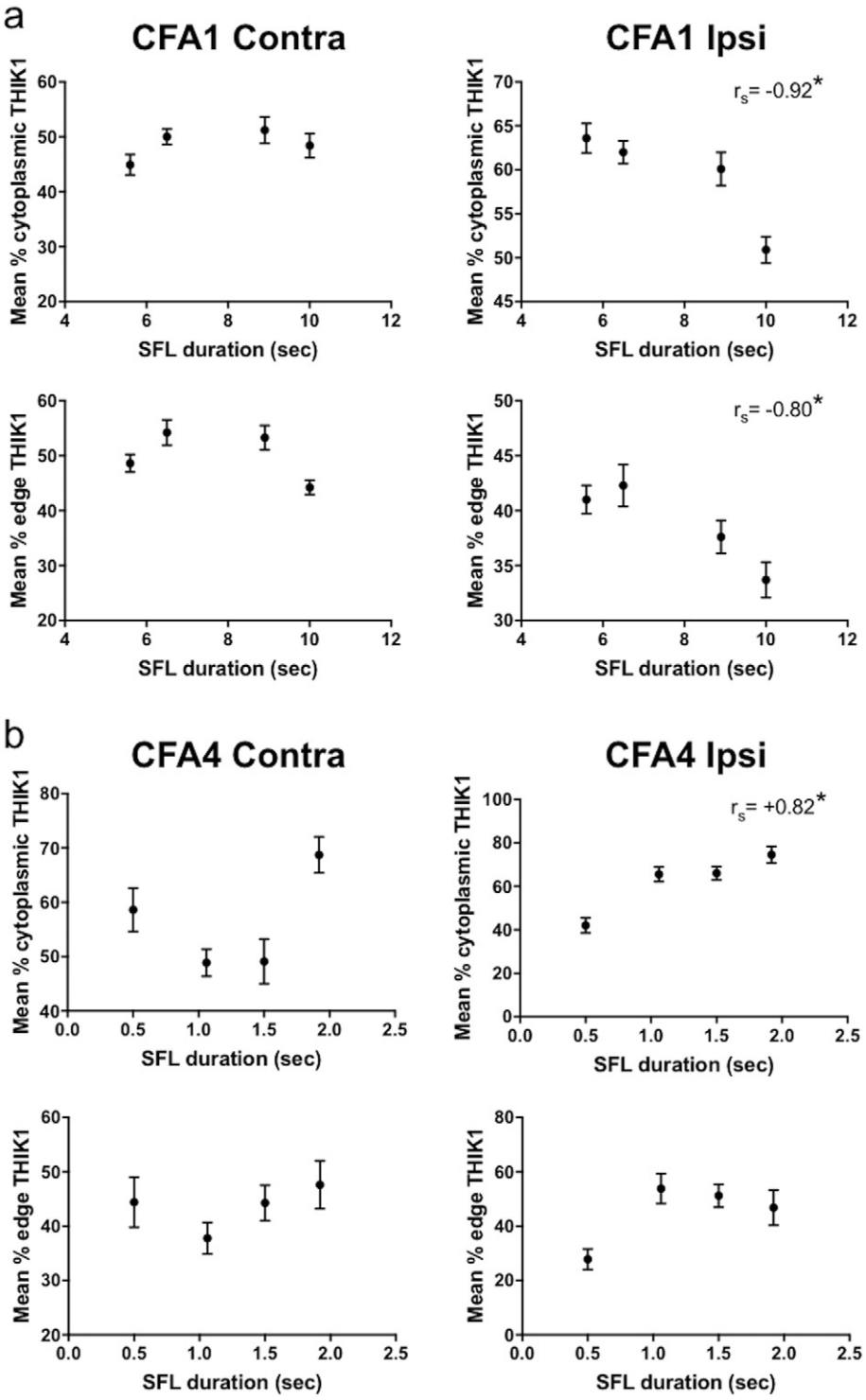

Fig. 7. THIK1 correlations with spontaneous foot lifting (SFL) during inflammation in small neurons SFL duration (in *sec*) recorded just prior to DRG removal plotted against THIK1 mean cytoplasmic %intensities and edge %intensities (±SEM) after inflammation induced by CFA injection contralaterally (Contra) and ipsilaterally (Ipsi). Each dot represents the mean ± SEM of 4 rats. (**a**) At CFA1 ipsilateral both THIK1 cytoplasmic and edge mean immunointensities were linearly and negatively correlated with SFL duration only for small neurons. Significance level was $^*p < 0.05$. (**b**) At CFA4 ipsilateral THIK1 cytoplasmic mean immunointensities were linearly and positively correlated with SFL duration for small neurons. Significance level was $^*p < 0.05$. No correlation was observed with edge mean immunointensities.

immunostained for THIK1, albeit the %intensities in these two groups are lower than in small neurons. Considering that medium and large size neurons include Aδ and Aβ nociceptors respectively (Lawson, 2002; Lawson and Waddell, 1991), it is possible that these are the THIK1 + medium and large neurons we observed. Considering this and the known sensory properties of DRG neurons classed by size, THIK1 could play a role in nociception. Nevertheless, it is possible that THIK1 is also expressed by other sensory subpopulations, like the C-low threshold mechanoreceptors (C-LTMs) or A-fiber LTMs. To address this question, we examined the co-expression of THIK1 with known phenotypic markers of DRG neurons.

First, we studied the co-localization of THIK1 with the Neurofilament of 200 kDa (NF200) using the monoclonal antibody RT97 that stains only myelinated A-fibers (both LTMs and Aβ and Aδ nociceptors)

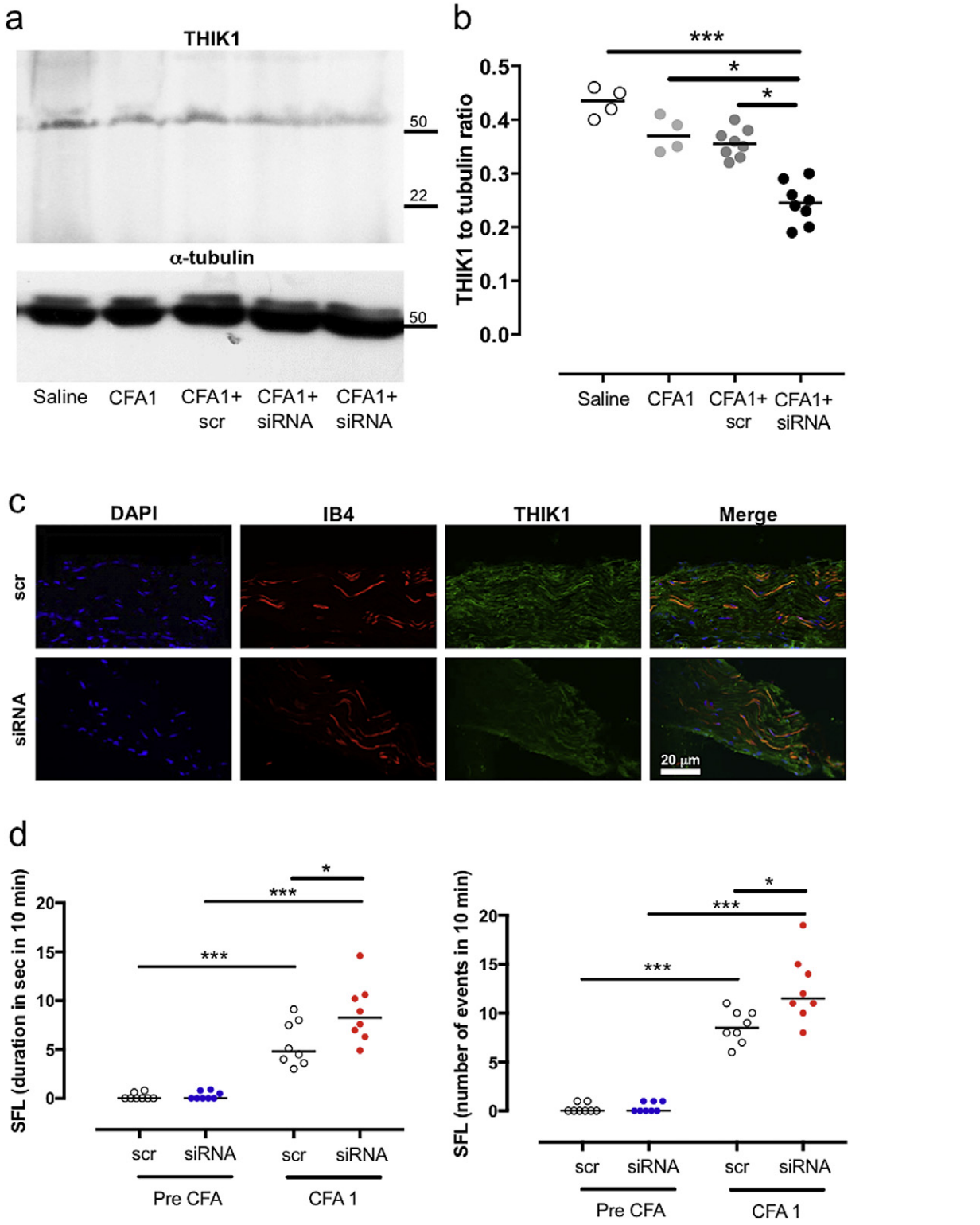

Fig. 8. Effects on spontaneous foot lifting (SFL) of THIK1 knockdown. THIK1 siRNA or scrambled siRNA was injected intradermally into the plantar region of one hind foot 3 days prior to CFA intradermal injection in the same area. (**a**) Western blots of skin tissue at the site of siRNA/scr injection. siRNA, not scr, treatment reduced THIK1 expression. (**b**) Quantitation of THIK1 protein levels shows a significant reduction of the channel with siRNA compared to saline and scr treated rats. CFA alone and CFA with scr showed a modest (statistically non-significant) reduction in THIK1 compared to saline. (**c**) In the nerve innervating the plantar skin 5–10 mm from the skin, THIK1 was knocked down, as shown by decreased fiber THIK1 immunostaining after siRNA. (**d**) Neither SFL duration (left) or number of events (right) was increased by THIK1 knockdown (siRNA) or scr pre CFA. After CFA, both SFL duration and number of events were increased ($p < 0.001$, Mann Whitney) in both scr and siRNA rats; SFL was significantly greater in THIK1 siRNA rats, compared with scr ($p < 0.05$). (For interpretation of the references to colour in this figure legend, the reader is referred to the web version of this article.)

(Lawson, 2002; Lawson et al., 1984; Perry et al., 1991). As shown in Fig. 3, cytoplasmic THIK1 is usually low or absent in most NF200+ neurons, although a degree of edge THIK1 staining is observed in most NF200+ neurons. Although edge staining is a better reflection of functional channels, the absence of cytoplasmic staining in neurofilament-rich neurons suggests total cell THIK1 to be low in myelinated A-fibers and we thus

speculate the functional significance of THIK1 in these fibers may be small. However, a full-scale study of THIK1 contribution to Em would be needed to confirm this hypothesis. To further clarify the sensory expression of THIK1, we next used 2 markers of nociceptors: IB4-binding and expression of trkA.

IB4 is a plant lectin that selectively binds to versican in a subpopulation of DRG neurons (Bogen et al., 2015). IB4-binding neurons (IB4+) are very small (≤300 μm^2), NF200-, non-peptidergic C-nociceptors that express high levels of Nav1.9 (Fang et al., 2006). IB4+ neurons innervate skin where they penetrate into the epidermis and express mrgprD (Zylka et al., 2005). IB4+ neurons include heat sensitive C-nociceptors (Fang et al., 2006) and 95% of them express the K2P channel TREK2, which limits spontaneous pain (Acosta et al., 2014). Thus, the co-localization of THIK1 and IB4 suggests that this K2P channel may be involved in pain perception mediated by this neuronal subpopulation. However the correlation between THIK1 staining and IB4-binding is relatively weak, meaning that the role of THIK1 in IB4+ neurons requires further examination.

Intriguingly, THIK1 staining was positively and strongly correlated with trkA, the high affinity receptor for NGF (see (Jankowski and Koerber, 2010) and references therein). *In vivo* studies have demonstrated that trkA is expressed almost exclusively by nociceptors, albeit there are also low levels in some C and Aδ-LTMs (Fang et al., 2005). The fact that only a very few trkA+/THIK1+ large neurons were observed, and none of these were SP+, seems to suggest that medium and large THIK1+ neurons are likely LTMs rather than A-nociceptors. In fact, all THIK1+/SP+ neurons were small making them peptidergic C-nociceptors. NGF activation of trkA in peripheral nociceptors plays a central role in initiating and sustaining heat and mechanical hyperalgesia following inflammation (Lewin and Nykjaer, 2014; McMahon, 1996; Stucky et al., 1999). Interestingly, blockage of trkA using monoclonal antibodies ameliorates CFA-induced electrophysiological changes in nociceptors (Djouhri et al., 2001) and also attenuates pain associated with inflammatory arthritis (Ashraf et al., 2016). Finally, the NGF/trkA system is essential for the establishment of neural networks for interoception, homeostasis and emotional responses (Anand, 2004; Indo, 2012). These facts support the notion that THIK1+ neurons are likely to be involved in NGF/trkA-mediated nociception.

4.2. THIK1 and inflammation

Following on from our previous study, we show here that THIK1 protein levels closely mimic the changes reported for THIK1 mRNA levels after CFA-induced cutaneous inflammation (Marsh et al., 2012). The pattern of expression was somewhat similar: a bilateral drop at CFA1 and at CFA4 at the edge of small neurons, with little or no change for medium and large neurons either at cytoplasmic or edge levels, in both instances compared to normal. Lowering the expression of K2P channels or inhibiting its activity will result in a reduced K^+ leakage and therefore a more depolarized Em. In turn, this depolarization makes nociceptors more excitable as they are closer to the threshold of activation for Nav1.7 channels, facilitating firing of action potentials and causing pain (Dib-Hajj et al., 2007; Dib-Hajj et al., 2008).

Although a relatively modest reduction, we demonstrated that THIK1 expression significantly dropped at CFA1 (cytoplasmic and edge) and CFA4 (edge) in small neurons only. There is a recovery in the cytoplasmic expression of THIK1 in small neurons at CFA4, but the levels at the edge remain consistently lowered compared to contralateral and normal. Assuming that the edge %intensities are more likely to reflect functional channels, this finding may indicate that THIK1 involvement in inflammatory pain continues through from CFA1 to CFA4. In this context, the lack of change in expression of THIK1 in medium and large neurons at CFA1 and CFA4 points to a more influential role for the channel in C-fiber like neurons. Therefore, the determinants of THIK1 expression differ between large and small neurons, as is also the case for other ion channels in DRG neurons (Acosta et al., 2012). We must point out that a larger sample of small neurons was analyzed compared to medium and large. This is a result of the larger proportion of small *vs.* medium/large neurons in the mid-sections of L5 DRG and the fact that we measured only neurons with a visible nuclei and the same number of sections per rat. Thus, this reflects the actual subpopulations within the DRG. However, given the high range of channel expression, and relatively small change in expression within small neurons following inflammation, it is plausible that a larger sample of medium and large neurons may reveal alterations to THIK1 expression. Notwithstanding this and considering the lower baseline channel expression in larger neurons and the homoscedasticity of the data, we do not believe this to be the case.

In terms of the bilateral changes in THIK1 expression seen with inflammation it must be noted that growing evidence suggests that systemic (*i.e.* circulating) inflammatory influences may reach and affect all DRGs (*e.g.* see (Jancalek et al., 2011; Koltzenburg, 1999; Marsh et al., 2012)). These influences have been shown to result from circulating pro-inflammatory mediators (*i.e.* cytokines) and/or hormones, all released in response to inflammation or pain (Milligan et al., 2003; Uceyler et al., 2009).

Paired with our findings that a large proportion of THIK1+ neurons are likely nociceptors (co-expressing trkA and binding IB4) this is consistent with this K2P channel playing a role in inflammatory pain.

In our previous study demonstrating K2P mRNA changes at CFA1, we found THIK1 and THIK2 to exhibit the greatest change. However, non-significant changes were observed for TRESK, TASK1, TASK2, TASK3 and TWIK2 (Marsh et al., 2012). Nonetheless, there is evidence for the involvement of other K2P channels in inflammation. For instance, Kollert et al. showed that excitation of nociceptors by the inflammatory pain mediator lysophosphatidic acid was attenuated by activation of TRESK channels (Kollert et al., 2015). Similarly, colon inflammation reduced TREK1 mRNA levels and TREK-like channels activity probably increasing DRG neurons mechanosensitivity (La and Gebhart, 2011). Thus, our findings add THIK1 to the list of K2P's probably implicated in inflammatory pain.

4.3. THIK1 and spontaneous pain

It is believed changes in Em are likely to contribute to changes in spontaneous firing (SF) and sensitivity of C-fibers, corroborated by the findings that neuropathic pain patients with spontaneous pain have more SF than those without spontaneous pain (Kleggetveit et al., 2012). Accordingly, the K2Ps with greatest influence on Em are theorised to carry greatest impact towards development of spontaneous pain. Interestingly, we observed that mean overall cytoplasmic and more importantly, edge THIK1%intensities in small neurons at CFA1 correlate significantly and negatively with SFL duration. It is believed that lower K2P expression would translate into lowered K^+ leakage, thus causing membrane potential depolarization. This, in turn, would result in a facilitation of spontaneous firing by nociceptors. Unfortunately no data on the contribution of THIK1 to Em in DRG neurons exist. This fact makes it difficult to ascertain the exact contribution of THIK1 to spontaneous pain at CFA1. Notwithstanding this, our immunostaining shows that THIK1 is expressed by almost all small neurons (likely C-fiber nociceptors) and by large subpopulations of medium and large neurons as well. This is somewhat similar to what has previously been observed for other K2Ps involved in pain such as TRAAK and TRESK, indeed suggesting a role for THIK1 in nociception and pain processing. Further to this, our finding that selectively knocking down THIK1 *in vivo* resulted in a moderately longer duration of SFL lends credence to a possible role of THIK1 in spontaneous pain.

The positive correlations we observed at CFA4 are intriguing. However, in the absence of concrete experimental evidence, we can only speculate about its physiological meaning. In the case of correlations of SFL with mean THIK1 edge %intensities, it is likely that increased

edge expression of THIK1 would equate to increased K^+ leakage from the cell (unless inhibition or inactivation of channels occurs). Perhaps some neurons increase the synthesis of THIK1 as part of a delayed response to inflammation. Such a response may attempt a hyperpolarization of Em and a reduction in neuronal excitability that would ultimately attenuate pain. However, SFL is much reduced at CFA4, thus whether THIK1 plays a role in spontaneous pain at this time requires more detailed studies.

Considering our observed expression of THIK1 in suggested nociceptor-like neurons and the results from our siRNA *in vivo* experiments, correlations observed between THIK1 %intensities and SFL duration are interesting. However, in view of the dominating influence and potential up regulation of more abundant K2Ps in the DRG (like TREK2 or TRESK), we propose that THIK1 may be a contributor rather than the most important player in the context of spontaneous pain.

5. Conclusion

This study highlights the relevant participation of K^+ channels in the genesis and maintenance of inflammatory and pathological pain. The magnitude and nature of the K^+ channel involvement in pain states will vary depending on the biophysical properties and localization to specific subpopulations of DRG neurons. These channels are postulated to inhibit peripheral excitability by limiting or impeding AP initiation at peripheral nerve terminals, thus reducing conduction fidelity across the axon, or limiting neurotransmitter release at central terminals. This opens up new therapeutic possibilities. Indeed, peripheral application of K^+ channel openers invariably decreases DRG excitability, whereas K^+ channel blockers augment firing (reviewed by (Busserolles et al., 2016; Tsantoulas and McMahon, 2014)). Neurons of all size express THIK1 although high IB4 and trkA co-expression suggest physiological importance within nociceptors. Given that cutaneous inflammation regulates THIK1 expression in small neurons, where channel expression is greatest, THIK1 may carry biggest influence within C-nociceptors. Thus, this study suggests that THIK1 may contribute to pain processing in the DRG making it a potential new therapeutic target alongside other K2Ps.

Funding

The Agencia Nacional de Promoción Científica y Tecnológica (Argentina) [grant number PICT-2014-0651 to C.A.] supported this work. W.H. received a student scholarship granted by the Nuffield Foundation (UK).

Acknowledgements

We thank Mabel Foscolo for technical help and Prof. Sally N. Lawson for the kind donation of plasmids for K2P channels and for helpful discussions and comments on the manuscript. The authors have no conflict of interest to declare.

Appendix A. Supplementary data

Supplementary data to this article can be found online at http://dx.doi.org/10.1016/j.mcn.2017.06.010.

References

Acosta, C., McMullan, S., Djouhri, L., Gao, L., Watkins, R., Berry, C., Dempsey, K., Lawson, S.N., 2012. HCN1 and HCN2 in rat DRG neurons: levels in nociceptors and non-nociceptors, NT3-dependence and influence of CFA-induced skin inflammation on HCN2 and NT3 expression. PLoS One 7, e50442.

Acosta, C., Djouhri, L., Watkins, R., Berry, C., Bromage, K., Lawson, S.N., 2014. TREK2 expressed selectively in IB4-binding C-fiber nociceptors hyperpolarizes their membrane potentials and limits spontaneous pain. J. Neurosci. 34, 1494–1509.

Anand, P., 2004. Neurotrophic factors and their receptors in human sensory neuropathies. Prog. Brain Res. 146, 477–492.

Asante, C., Wallace, V., Dickenson, A., 2009. Formalin-induced behavioural hypersensitivity and neuronal hyperexcitability are mediated by rapid protein synthesis at the spinal level. Mol Pain. 5, 27.

Ashraf, S., Bouhana, K.S., Pheneger, J., Andrews, S.W., Walsh, D.A., 2016. Selective inhibition of tropomyosin-receptor-kinase A (TrkA) reduces pain and joint damage in two rat models of inflammatory arthritis. Arthritis Res. Ther. 18, 97.

Bogen, O., Bender, O., Lowe, J., Blenau, W., Thevis, B., Schroder, W., Margolis, R.U., Levine, J.D., Hucho, F., 2015. Neuronally produced versican V2 renders C-fiber nociceptors IB4 -positive. J. Neurochem. 134, 147–155.

Bryan Jr., R.M., You, J., Phillips, S.C., Andresen, J.J., Lloyd, E.E., Rogers, P.A., Dryer, S.E., Marrelli, S.P., 2006. Evidence for two-pore domain potassium channels in rat cerebral arteries. Am. J. Physiol. Heart Circ. Physiol. 291, H770–H780.

Busserolles, J., Tsantoulas, C., Eschalier, A., Lopez Garcia, J.A., 2016. Potassium channels in neuropathic pain: advances, challenges, and emerging ideas. Pain 157 (Suppl. 1), S7–14.

Dib-Hajj, S.D., Cummins, T.R., Black, J.A., Waxman, S.G., 2007. From genes to pain: Na v 1.7 and human pain disorders. Trends Neurosci. 30, 555–563.

Dib-Hajj, S.D., Yang, Y., Waxman, S.G., 2008. Genetics and molecular pathophysiology of Na(v)1.7-related pain syndromes. Adv. Genet. 63, 85–110.

Djouhri, L., Dawbarn, D., Robertson, A., Newton, R., Lawson, S.N., 2001. Time course and nerve growth factor dependence of inflammation-induced alterations in electrophysiological membrane properties in nociceptive primary afferent neurons. J. Neurosci. 21, 8722–8733.

Djouhri, L., Koutsikou, S., Fang, X., McMullan, S., Lawson, S.N., 2006. Spontaneous pain, both neuropathic and inflammatory, is related to frequency of spontaneous firing in intact C-fiber nociceptors. J. Neurosci. 26, 1281–1292.

Djouhri, L., Fang, X., Koutsikou, S., Lawson, S.N., 2012. Partial nerve injury induces electrophysiological changes in conducting (uninjured) nociceptive and nonnociceptive DRG neurons: possible relationships to aspects of peripheral neuropathic pain and paresthesias. Pain 153, 1824–1836.

Du, X., Hao, H., Gigout, S., Huang, D., Yang, Y., Li, L., Wang, C., Sundt, D., Jaffe, D.B., Zhang, H., Gamper, N., 2014. Control of somatic membrane potential in nociceptive neurons and its implications for peripheral nociceptive transmission. Pain 155, 2306–2322.

Enyedi, P., Czirjak, G., 2010. Molecular background of leak K^+ currents: two-pore domain potassium channels. Physiol. Rev. 90, 559–605.

Fang, X., Djouhri, L., McMullan, S., Berry, C., Okuse, K., Waxman, S.G., Lawson, S.N., 2005. trkA is expressed in nociceptive neurons and influences electrophysiological properties *via* Nav1.8 expression in rapidly conducting nociceptors. J. Neurosci. 25, 4868–4878.

Fang, X., Djouhri, L., McMullan, S., Berry, C., Waxman, S.G., Okuse, K., Lawson, S.N., 2006. Intense isolectin-B4 binding in rat dorsal root ganglion neurons distinguishes C-fiber nociceptors with broad action potentials and high Nav1.9 expression. J. Neurosci. 26, 7281–7292.

Indo, Y., 2012. Nerve growth factor and the physiology of pain: lessons from congenital insensitivity to pain with anhidrosis. Clin. Genet. 82, 341–350.

Ishii, H., Nakajo, K., Yanagawa, Y., Kubo, Y., 2010. Identification and characterization of Cs(+) -permeable K(+) channel current in mouse cerebellar Purkinje cells in lobules 9 and 10 evoked by molecular layer stimulation. Eur. J. Neurosci. 32, 736–748.

Jancalek, R., Svizenska, I., Klusakova, I., Dubovy, P., 2011. Bilateral changes of IL-10 protein in lumbar and cervical dorsal root ganglia following proximal and distal chronic constriction injury of peripheral nerve. Neurosci. Lett. 501, 86–91.

Jankowski, M.P., Koerber, H.R., 2010. Neurotrophic Factors and Nociceptor Sensitization.

Kang, D., Hogan, J.O., Kim, D., 2014. THIK-1 (K2P13.1) is a small-conductance background K(+) channel in rat trigeminal ganglion neurons. Pflugers Arch. 466, 1289–1300.

Kashiba, H., Ueda, Y., Senba, E., 1996. Coexpression of preprotachykinin-A, alpha-calcitonin gene-related peptide, somatostatin, and neurotrophin receptor family messenger RNAs in rat dorsal root ganglion neurons. Neuroscience 70 (1), 179–189.

Kleggetveit, I.P., Namer, B., Schmidt, R., Helas, T., Ruckel, M., Orstavik, K., Schmelz, M., Jorum, E., 2012. High spontaneous activity of C-nociceptors in painful polyneuropathy. Pain 153, 2040–2047.

Kollert, S., Dombert, B., Doring, F., Wischmeyer, E., 2015. Activation of TRESK channels by the inflammatory mediator lysophosphatidic acid balances nociceptive signalling. Sci. Rep. 5, 12548.

Koltzenburg, M., 1999. The changing sensitivity in the life of the nociceptor. Pain Suppl. 6, S93–102.

La, J.H., Gebhart, G.F., 2011. Colitis decreases mechanosensitive K2P channel expression and function in mouse colon sensory neurons. Am. J. Physiol. Gastrointest. Liver Physiol. 301, G165–G174.

Lafreniere, R.G., Cader, M.Z., Poulin, J.F., Andres-Enguix, I., Simoneau, M., Gupta, N., Boisvert, K., Lafreniere, F., McLaughlan, S., Dube, M.P., Marcinkiewicz, M.M., Ramagopalan, S., Ansorge, O., Brais, B., Sequeiros, J., Pereira-Monteiro, J.M., Griffiths, L.R., Tucker, S.J., Ebers, G., Rouleau, G.A., 2010. A dominant-negative mutation in the TRESK potassium channel is linked to familial migraine with aura. Nat. Med. 16, 1157–1160.

Lawson, S.N., 2002. Phenotype and function of somatic primary afferent nociceptive neurones with C-, Adelta- or Aalpha/beta-fibres. Exp. Physiol. 87, 239–244.

Lawson, S.N., Waddell, P.J., 1991. Soma neurofilament immunoreactivity is related to cell size and fibre conduction velocity in rat primary sensory neurons. J. Physiol. 435, 41–63.

Lawson, S.N., Harper, A.A., Harper, E.I., Garson, J.A., Anderton, B.H., 1984. A monoclonal antibody against neurofilament protein specifically labels a subpopulation of rat sensory neurones. J. Comp. Neurol. 228, 263–272.

Lawson, S.N., Perry, M.J., Prabhakar, E., McCarthy, P.W., 1993. Primary sensory neurones: neurofilament, neuropeptides, and conduction velocity. Brain Res. Bull. 30, 239–243.

Lazarenko, R.M., Fortuna, M.G., Shi, Y., Mulkey, D.K., Takakura, A.C., Moreira, T.S., Guyenet, P.G., Bayliss, D.A., 2010. Anesthetic activation of central respiratory chemoreceptor neurons involves inhibition of a THIK-1-like background K(+) current. J. Neurosci. 30, 9324–9334.
Lewin, G.R., Nykjaer, A., 2014. Pro-neurotrophins, sortilin, and nociception. Eur. J. Neurosci. 39, 363–374.
Marsh, B., Acosta, C., Djouhri, L., Lawson, S.N., 2012. Leak K(+) channel mRNAs in dorsal root ganglia: relation to inflammation and spontaneous pain behaviour. Mol. Cell. Neurosci. 49, 375–386.
Mathie, A., Veale, E.L., 2015. Two-pore domain potassium channels: potential therapeutic targets for the treatment of pain. Pflugers Arch. 467, 931–943.
McCarthy, P., Lawson, S., 1989. Cell type and conduction velocity of primary sensory neurons with substance P-like immunoreactivity. Neuroscience 28 (3), 745–753.
McMahon, S.B., 1996. NGF as a mediator of inflammatory pain. Philos. Trans. R. Soc. Lond. B Biol. Sci. 351, 431–440.
Millan, M.J., 1999. The induction of pain: an integrative review. Prog. Neurobiol. 57, 1–164.
Milligan, E.D., Twining, C., Chacur, M., Biedenkapp, J., O'Connor, K., Poole, S., Tracey, K., Martin, D., Maier, S.F., Watkins, L.R., 2003. Spinal glia and proinflammatory cytokines mediate mirror-image neuropathic pain in rats. J. Neurosci. 23, 1026–1040.
Ocana, M., Cendan, C.M., Cobos, E.J., Entrena, J.M., Baeyens, J.M., 2004. Potassium channels and pain: present realities and future opportunities. Eur. J. Pharmacol. 500, 203–219.
Parekh, A., Campbell, A.J., Djouhri, L., Fang, X., McMullan, S., Berry, C., Acosta, C., Lawson, S.N., 2010. Immunostaining for the alpha3 isoform of the Na^+/K^+-ATPase is selective for functionally identified muscle spindle afferents *in vivo*. J. Physiol. 588, 4131–4143.
Pereira, V., Busserolles, J., Christin, M., Devilliers, M., Poupon, L., Legha, W., Alloui, A., Aissouni, Y., Bourinet, E., Lesage, F., Eschalier, A., Lazdunski, M., Noel, J., 2014. Role of the TREK2 potassium channel in cold and warm thermosensation and in pain perception. Pain 155, 2534–2544.
Perry, M.J., Lawson, S.N., Robertson, J., 1991. Neurofilament immunoreactivity in populations of rat primary afferent neurons: a quantitative study of phosphorylated and non-phosphorylated subunits. J. Neurocytol. 20, 746–758.
Radtke, C., Akiyama, Y., Lankford, K.L., Vogt, P.M., Krause, D.S., Kocsis, J.D., 2005. Integration of engrafted Schwann cells into injured peripheral nerve: axonal association and nodal formation on regenerated axons. Neurosci. Lett. 387 (2), 85–89.
Rajan, S., Wischmeyer, E., Karschin, C., Preisig-Muller, R., Grzeschik, K.H., Daut, J., Karschin, A., Derst, C., 2001. THIK-1 and THIK-2, a novel subfamily of tandem pore domain K^+ channels. J. Biol. Chem. 276, 7302–7311.
Stefanini, M., De Martino, C., Zamboni, L., 1967. Fixation of ejaculated spermatozoa for electron microscopy. Nature 216, 173–174.
Stucky, C.L., Koltzenburg, M., Schneider, M., Engle, M.G., Albers, K.M., Davis, B.M., 1999. Overexpression of nerve growth factor in skin selectively affects the survival and functional properties of nociceptors. J. Neurosci. 19, 8509–8516.
Theilig, F., Goranova, I., Hirsch, J.R., Wieske, M., Unsal, S., Bachmann, S., Veh, R.W., Derst, C., 2008. Cellular localization of THIK-1 (K(2P)13.1) and THIK-2 (K(2P)12.1) K channels in the mammalian kidney. Cell. Physiol. Biochem. 21, 63–74.
Tsantoulas, C., 2015. Emerging potassium channel targets for the treatment of pain. Curr. Opin. Support. Palliat. Care 9, 147–154.
Tsantoulas, C., McMahon, S.B., 2014. Opening paths to novel analgesics: the role of potassium channels in chronic pain. Trends Neurosci. 37, 146–158.
Tulleuda, A., Cokic, B., Callejo, G., Saiani, B., Serra, J., Gasull, X., 2011. TRESK channel contribution to nociceptive sensory neurons excitability: modulation by nerve injury. Mol. Pain 7, 30.
Uceyler, N., Schafers, M., Sommer, C., 2009. Mode of action of cytokines on nociceptive neurons. Exp. Brain Res. 196, 67–78.
Usoskin, D., Furlan, A., Islam, S., Abdo, H., Lonnerberg, P., Lou, D., Hjerling-Leffler, J., Haeggstrom, J., Kharchenko, O., Kharchenko, P.V., Linnarsson, S., Ernfors, P., 2015. Unbiased classification of sensory neuron types by large-scale single-cell RNA sequencing. Nat. Neurosci. 18, 145–153.
Watkins, L.R., Maier, S.F., 2002. Beyond neurons: evidence that immune and glial cells contribute to pathological pain states. Physiol. Rev. 82, 981–1011.
Wood, J.N., 2007. Ion channels in analgesia research. Handb. Exp. Pharmacol. 329–358.
Wu, G., Ringkamp, M., Hartke, T.V., Murinson, B.B., Campbell, J.N., Griffin, J.W., Meyer, R.A., 2001. Early onset of spontaneous activity in uninjured C-fiber nociceptors after injury to neighboring nerve fibers. J. Neurosci. 21, RC140.
Wu, G., Ringkamp, M., Murinson, B.B., Pogatzki, E.M., Hartke, T.V., Weerahandi, H.M., Campbell, J.N., Griffin, J.W., Meyer, R.A., 2002. Degeneration of myelinated efferent fibers induces spontaneous activity in uninjured C-fiber afferents. J. Neurosci. 22, 7746–7753.
Wu, K., Zippin, J., Huron, D., Kamenetsky, M., Hengst, U., Buck, J., Levin, L., Jaffrey, S., 2006. Soluble adenylyl cyclase is required for netrin-1 signaling in nerve growth cones. Nat Neurosci. 9, 1257–1264.
Yoon, Y.W., Na, H.S., Chung, J.M., 1996. Contributions of injured and intact afferents to neuropathic pain in an experimental rat model. Pain 64, 27–36.
Zylka, M.J., Rice, F.L., Anderson, D.J., 2005. Topographically distinct epidermal nociceptive circuits revealed by axonal tracers targeted to Mrgprd. Neuron 45, 17–25.